

The inception of pulsed discharges in air: simulations in background fields above and below breakdown

Anbang Sun¹, Jannis Teunissen¹, Ute Ebert^{1,2}

¹Centrum Wiskunde & Informatica (CWI), P.O. Box 94079, 1090 GB Amsterdam,
The Netherlands,

²Dept. Physics, Eindhoven Univ. Techn., The Netherlands,

E-mail: a.sun@cwi.nl

Abstract. We investigate discharge inception in air, in uniform background electric fields above and below the breakdown threshold. We perform 3D particle simulations that include a natural level of background ionization in the form of positive and O_2^- ions. When the electric field rises above the breakdown and the detachment threshold, which are similar in air, electrons can detach from O_2^- and start ionization avalanches. These avalanches together create one large discharge, in contrast to the ‘double-headed’ streamers found in many fluid simulations.

On the other hand, in background fields below breakdown, something must enhance the field sufficiently for a streamer to form. We use a strongly ionized seed of electrons and positive ions for this, with which we observe the growth of positive streamers. Negative streamers were not observed. Below breakdown, the inclusion of electron detachment does not change the results much, and we observe similar discharge development as in fluid simulations.

1. Introduction

Developments in pulsed power technology have increased the interest in pulsed discharges over the last two decades. These discharges now have a wide range of applications, for example, ozone generation [1, 2, 3, 4], gas and water cleaning [3, 5, 6], flow control and plasma assisted ignition and combustion [7]. Pulsed discharges appear also in thunderstorms and in high voltage technology for electricity networks.

Here, we focus on the initial development of such pulsed discharges in air at standard temperature and pressure. We consider two different cases for the background electric field. It is either globally above the breakdown threshold, or only locally due to some field enhancement. In the first case, ionization processes can take place in the whole volume. In the second case, the discharge grows only in the region above breakdown, forming a streamer discharge. Streamers are fast growing plasma filaments that can penetrate into non-ionized regions due the electric field enhancement at their tips. In addition, streamers play an essential role in natural discharges, since they pave the path for lightning and sprites. They have been studied in different gases and in different electric field configurations both experimentally [8, 9, 10, 11, 12, 13, 14] and numerically [15, 16, 17, 18, 19, 20, 21, 22, 23, 24].

The main objective of the current paper is to show that in air one needs to distinguish between background electric fields above and below the breakdown threshold. We will argue that an important reason for this distinction is the presence of background ionization. In atmospheric air, some background ionization is always present, due to radioactivity, cosmic and solar radiation. The free electrons that are generated quickly attach to molecules, to form negative ions. In dry air at a pressure of 1 bar, which we consider in this article, the dominant negative ion is O_2^- . If the electric field rises above a threshold, called the detachment field, electrons can again detach from these O_2^- ions [25]. Remarkably, the detachment field is very similar to the electrical breakdown field in air. So if the background field rises above the breakdown threshold, electrons can detach, and every detached electron can start an electron avalanche.

We want to emphasize that both detachment and photoionization are characteristic for nitrogen/oxygen mixtures. In pure gases or other mixtures they might be absent or much weaker, see e.g. [8]. Furthermore, in air at pressures below 100 mbar, O^- ions become more important. From these ions electrons can detach in fields much below breakdown [26, 27, 28].

We consider the inception of pulsed discharges in homogeneous background fields, far from electrodes or other charge accumulations. Such situations occur for example in thunderclouds [29, 30]. In our recent Geophysical Research Letter [31], we have used a 3D particle model to compare discharge formation in air at standard temperature and pressure with and without natural background ionization, in electric fields above the breakdown value. We also briefly introduced an analytic estimate for the ‘ionization screening time’, after which the electric field in the interior of a discharge is screened. In the present paper, we further elaborate on the contents of the letter [31], and focus

on the distinction between background fields above and below breakdown. Therefore, we present the evolution of discharges in fields both above and below the breakdown threshold, using the same simulation model as in [31].

The outline of the paper is as follows. In Section 2, we introduce the simulation model, and discuss electron detachment from background ionization. In Section 3, we present simulation results for a background electric field above the breakdown threshold. The formation of streamers in electric fields below the breakdown threshold is investigated in Section 4. We there test what kind of initial ionization can lead to the field enhancement required to start a streamer discharge.

2. The set-up of the MC particle model

In recent years, we have developed a 3D particle code of the PIC-MCC type [32] to study discharge inception. The reason for using a 3D particle model is that the start of discharges is often a stochastic process, that lacks cylindrical (or other) symmetry. In the model, electrons are tracked as particles. Ions are assumed to be immobile, and are included as densities. They only contribute to space charge effects. Neutral gas molecules provide a background that electrons can randomly collide with; they are included in the code as a random background of given density.

The simulations of the present paper are performed in dry air (80% N₂, 20% O₂) at 1 bar and 293 Kelvin. For the electrons, we include elastic, excitation, ionization and attachment collisions with the neutral gas molecules. We use the cross sections from the SIGLO database [33] and the null-collision method to select collisions [34], with isotropic scattering after every collision. We ignore electron-electron and electron-ion collisions, because the degree of ionization in a pulsed discharge in STP air is typically below 10⁻⁴, which is also the case in the simulations we perform.

Simulating a discharge with a 3D particle code is computationally expensive, especially as the discharge grows. This limits the simulations we can perform to the first nanoseconds of a discharge, during which the inception takes place. On this time scale, heating, recombination and multi-step excitation or ionization can be neglected.

2.1. Adaptive particle management

As the number of electrons in a typical discharge quickly rises to 10⁸ or more, so-called super-particles have to be used. Using super-particles with a fixed weight would induce significant stochastic errors, and therefore we employ ‘adaptive particle management’ as described in [35]. The weight of simulated particles can then be adjusted by merging or splitting them, and care is taken to not alter their properties in a systematic way. A particle i can only be merged with its closest neighbor j that also needs to be merged, with ‘closest’ defined as minimizing

$$d^2 = (\vec{x}_i - \vec{x}_j)^2 + \lambda^2 |v_i - v_j|^2, \quad (1)$$

where \vec{x} denotes the Cartesian position vector, v is the norm of the velocity and λ is a scaling factor that we set to one picosecond. A newly formed merged particle gets its velocity at random from one of the original particles, while its position is set to the weighted average position, see [35] for a comparison of different schemes to merge particles. We adjust the weights so that every cell of the grid (see below) contains at least 50 simulation particles. So if no more than 50 electrons are present in a cell, then each simulation particle represents a single electron. But where the electron density is high, with much more than 50 electrons in a cell, most simulation particles represent many electrons.

2.2. Adaptive Mesh Refinement for the electric field

In the particle code, the electric field is computed from the electric potential. The potential is computed by solving Poisson's equation with the charge density as the source term, using the HW3CRT solver from the FISHPACK library [36]. When space charge effects become important in a discharge, a grid fine enough to resolve the space charge structures has to be used. For streamer discharges, that are surrounded by a thin space charge layer, this means that a fine grid is required around the layer. In our simulations, we use the following criterion for the grid spacing

$$\Delta x < 1/\alpha(E), \quad (2)$$

where $\alpha(E)$ is the ionization coefficient, that describes the average number of ionizations a single electron will generate per unit length in a field of strength E . For air at 1 bar and in an electric field of 15 MV/m, a typical field for streamer tips, this gives $\Delta x \sim 5 \mu\text{m}$. Because a typical simulation domain measures at least a few mm in each direction, using such a fine grid everywhere is computationally infeasible. Therefore, we have implemented block-based adaptive mesh refinement, in the same way as in [37], although now in 3D. First, the electric potential is computed on a uniform, coarse grid. Then the rectangular area that contains the points at which the electric field is larger than some threshold is refined, by a factor of two. The electric potential in the refined rectangle is then computed by imposing Dirichlet boundary conditions interpolated from the coarse grid. This procedure is repeated with the refinement criterion given by equation (2).

For the simulation of streamer discharges, the block-based grid refinement strategy described above works relatively well, because high electric fields are present only in a small region. But for the simulation of discharges that spread out over the whole domain, as we will see in section 3, this type of grid refinement does not reduce the computational cost much.

2.3. Photoionization

Photoionization provides a non-local ionization mechanism in air. This is especially important for the propagation of positive streamers, that need a source of free electrons ahead of them to propagate. We use the same approach as in [38] and [39], where a

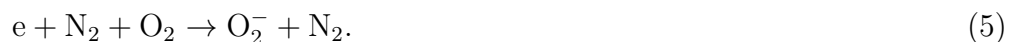
discrete, stochastic version of Zhelezniak's photoionization model [40] is implemented. In this model, the average density of ionizing photons S_{ph} produced at \vec{r} is given by

$$S_{\text{ph}}(\vec{r}) = S_{\text{ion}}(\vec{r}) \eta(E), \quad (3)$$

where S_{ion} represents the number of ionizations and $\eta(E)$ is an efficiency, estimated from experimental measurements, that depends on the local electric field E and the gas mixture. When an ionizing photon is generated, its place of absorption is determined using random numbers, and at that position an electron-ion pair is created. The average absorption distance is about 0.5 mm in air at 1 bar. For details about the implementation of the photoionization model we refer to [38].

2.4. Electron detachment from background ionization

In atmospheric air, there is always some background ionization present, due to radioactivity and cosmic or solar radiation. Previous discharges can also play a role, both in nature [41] and in the lab [9]. At standard temperature and pressure, the free electrons that are created by these sources attach to oxygen molecules mostly by three-body attachment [25]:



These negative ions have a longer life time than the electrons. Inside buildings, background ionization levels of $10^3 - 10^4 \text{ cm}^{-3}$ are typical, primarily due to the decay of radon, see [42] for a review. When O_2^- molecules collide with a neutral gas molecule, they can lose an electron. This can be regarded as the inverse of the reactions in Equations (4) and (5):



The rate constants for these detachment reactions can be related to the reduced electric field E/N and the number density of the neutrals. We use the rates given in [25]. For a given number density of the neutrals, we call the total rate at which electrons detach from O_2^- ions the *detachment rate*. Additionally, we call the inverse of the detachment rate the detachment time τ_D . In figure 1, the dependence of τ_D on the electric field strength is shown.

If during a simulation an electron has an attachment collision, then the electron is removed and an O_2^- ion is created at the electron's position. We currently consider only this type of negative ion, although O^- can also form due to dissociative attachment, mostly at lower pressures or higher electron energies, and many more ions can be generated by chemical reactions [27, 43].

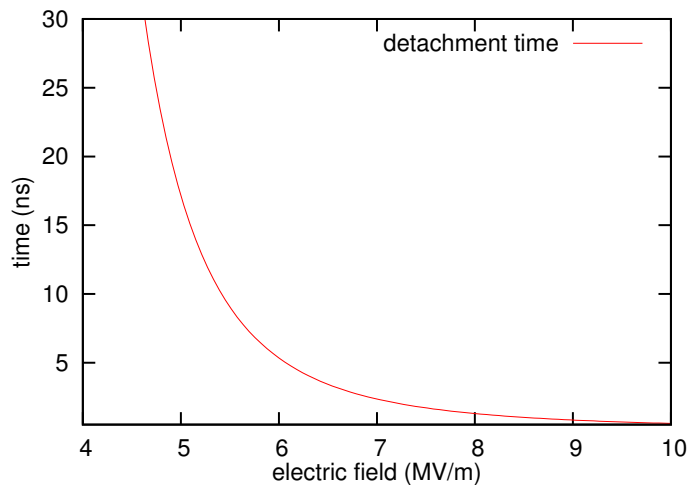


Figure 1. The detachment time τ_D as a function of the electric field strength in STP air. In higher fields, negative ions have a higher energy and drift faster, so they are more likely to lose an electron in a collision with a neutral molecule.

3. Discharges in background fields above breakdown

3.1. Previous work

Up to now, pulsed discharges in air have mainly been simulated with plasma fluid models [19, 44, 45, 46, 47, 48, 49], where the charged particles are approximated by densities. The most common fluid model assumes that the electrons drift, diffuse and react (ionize), with the coefficients for these processes determined by the local electric field strength. Typically cylindrical symmetry is assumed, and therefore these fluid models need just two spatial coordinates, making them computationally much less expensive than our 3D particle code. Authors typically place some localized initial ionization in the domain to start a discharge [19, 47, 48, 49]. In background fields above the breakdown threshold, this ionization seed then develops into a ‘double-headed’ streamer, where both the positive and the negative end grow simultaneously. The effect of including natural background ionization (and detachment) has not been studied with these models.

However, including background ionization and detachment is very important for discharges in air above breakdown, as we have recently demonstrated in [31]. There we presented 3D particle simulations in a background field of 7 MV/m (where the breakdown field is 3 MV/m) with three different initial conditions: either only one electron, or one electron together with a background density of 10^3 O_2^- ions per cm^3 , or this background density alone without an initial electron. Our results showed that in the first case indeed a double-headed streamer emerged, while in both cases with a realistic background ion density, the discharge developed in a much more homogeneous manner: The natural background ionization together with the detachment reaction generates free electrons everywhere in the region above breakdown. As this is a stochastic process, the resulting discharge does not have cylindrical symmetry, which is why we use the 3D

particle model introduced in section 2. Simulations with a background density of 10^4 O_2^- ions per cm^3 in background fields of 6 MV/m are presented in section 3.3.

3.2. Boundary conditions for the simulations above breakdown

In this section, we present new simulation results for a discharge developing from a natural level of background ionization of O_2^- ions in a field of 6 MV/m, well above breakdown. We want to simulate the development of a discharge that is not in contact with physical boundaries, like electrodes. This is achieved by using periodic boundary conditions in the x and y direction, while limiting the region where background ionization is present in the z direction. In other words, we simulate the development of a thick discharge layer growing from background ionization. The elongated computational domain is shown in Figure 2, where the region with background ionization is shaded green. At the top and bottom of the domain we apply Neumann boundary conditions for the electric potential, thereby creating a uniform background field E_0 of 6 MV/m.

We remark that in the GRL [31] we were less careful with the boundary conditions and used something similar to Fig. 6. As the complete pre-ionized region becomes electrically screened, the boundary of the pre-ionized region induced distortions of the electric field.

We do not use grid refinement to calculate the generated electric field in this simulation as grid refinement would be required nearly everywhere in the pre-ionized region. The static grid contains $100 \times 100 \times 535$ cells, with a cell length of 15 μm . The domain length is chosen in such a manner that the discharge does not reach its boundaries within the time simulated.

3.3. Simulated discharge evolution

Figure 3 shows the evolution of the electron density and the electric field in four time steps between 4.5 ns and 5.4 ns. The evolution of the discharge can be characterized as follows. First, free electrons appear due to detachment. As can be seen in figure 1, the characteristic detachment time in a field of 6 MV/m is about 5 ns. Then these free electrons start electron avalanches, that quickly grow due to impact ionization. The growing avalanches also produce photoionization, thereby starting additional avalanches. Eventually, many avalanches emerge in the simulation domain.

After about 5 ns, space charge effects start to become important, causing the electric field to increase locally up to ~ 9 MV/m while decreasing elsewhere. These space charge effects increase in magnitude until the simulation stops at 5.4 ns. The distribution of the electric field values is shown in figure 4. After 4.5 ns almost the complete system is still at the background field of 6 MV/m, while about 8% of the volume has a field lower than the breakdown value of 3 MV/m after 5.4 ns.

Figure 5 shows the distribution of electric fields in the simulation in another manner; it shows the electric field averaged over the horizontal planes intersecting Figure 3 and plotted as a function of the longitudinal coordinate. The screening of the electric field

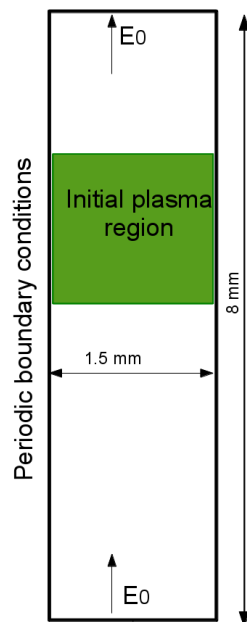


Figure 2. Schematic of the computational domain in the 3D overvolted simulations. Periodic boundary conditions are used in the two lateral directions. At the top and bottom of the domain, the electric field is fixed to a value E_0 of 6 MV/m. Initially, background ionization is present in the green region.

occurs in a ‘noisy’ way, and the electric field varies significantly inside the discharge. This is not so surprising, as initially only about 45 negative ions (O_2^-) are present. With these ions randomly placed in a volume of 4.5 mm^3 , we do not expect a discharge homogeneously filled with ionization.

The simulation stops when there are too many simulation particles for the computer’s memory, which happened here at about $3 \cdot 10^7$ particles.

3.4. Conclusions and further work

Two conclusions can be drawn from these results:

First, the simulations show a rather global breakdown in the pre-ionized region, instead of a double-headed streamer. This is due to the inclusion of a natural background of oxygen ions and the electron detachment reaction from these ions in a field approximately above the breakdown value.

Second, the breakdown is not completely uniform either, but shows a competition of local streamer formation and global breakdown that creates a certain patchiness of ionization and makes the electric field screening noisy.

A detailed analysis of these phenomena and their relation to the concept of an ionization screening time [31] will be discussed in a forthcoming paper [50].

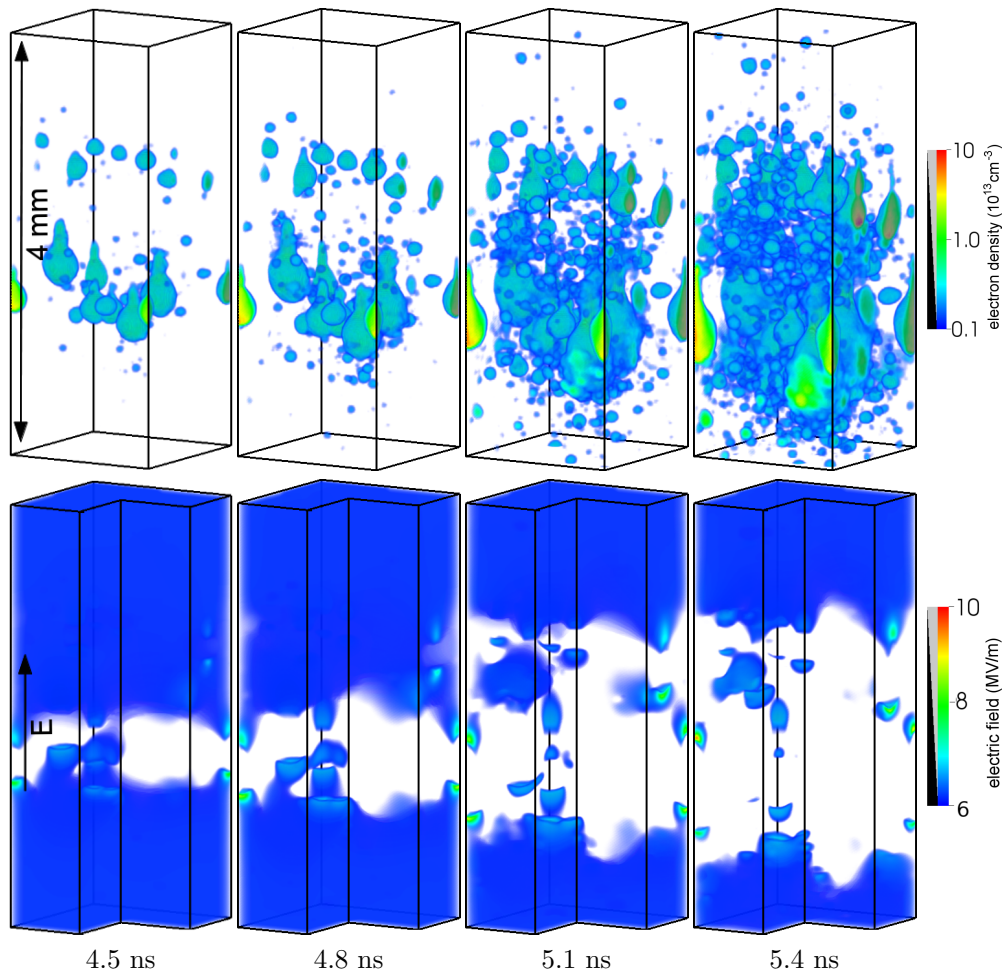


Figure 3. The time evolution of the electron density (top row) and of the electric field (bottom row). Background ionization is initially present in the green region of Figure 2, in the form of O_2^- and positive ions, both with a density of 10^4 cm^{-3} . The gas is dry air at 1 bar and 293 K in an upward directed homogeneous electric field of 6 MV/m, which is about two times the breakdown field. The domain between 2 mm and 6 mm in the vertical direction of Figure 2 is shown. The figures were generated using volume rendering, and the opacity is shown next to the colorbar; black indicates transparency. For the figures in the second row, a quarter of the domain is removed to show the inner structures of the electric field.

4. Discharges in background fields below breakdown

4.1. Previous work

In this section, we investigate streamer formation in background electric fields below the breakdown threshold. Will the 3D particle model together with background ionization and electron detachment also lead to major deviations from previous results derived with a 2D fluid model?

In such a simulation, of course, the field has to exceed the breakdown threshold in

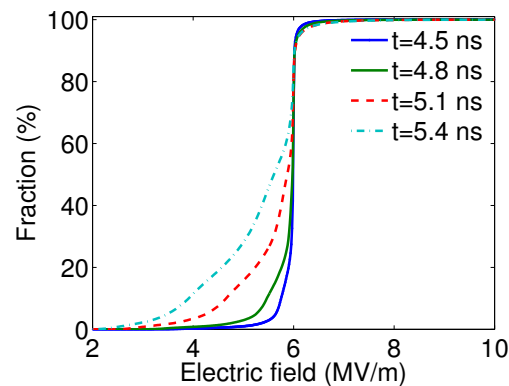


Figure 4. The volume fraction with a field smaller than E as a function of E . We evaluate the green domain shown in figure 3.

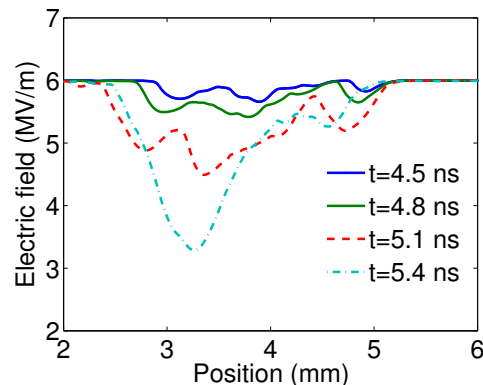


Figure 5. The screened electric field at different times. The electric field was averaged over planes perpendicular to the background field in Figure 3 and plotted as a function of the coordinate parallel to the field.

some region, otherwise a discharge cannot start. An electric field that is only locally above breakdown can be generated in several ways. In experiments, such a field can be created by sharp electrodes, to which a voltage is applied. Another possibility is that a conducting or polarizable object floats in a field below breakdown; examples include dust, water droplets or ice crystals. At the endpoints of the object, the field will increase, especially if the object has an elongated shape along the direction of the background field. Yet another way to start a discharge is to have a strongly ionized region that therefore acts as a conductor. This typically requires electrons, as they have a much higher mobility than ions.

Such ionized seeds have been commonly used in fluid simulations of streamers for the past 30 years, often without explicit mentioning. Liu *et al* [51] used an ionized column as a substitute of a droplet or ice particle to start streamer discharges. Assuming that the ionized column was perfectly conducting and had a typical streamer radius, they presented an estimate on its minimal length to provide sufficient field enhancement

[51, 52]. A positive streamer was able to form if the electric field at the tip can be enhanced to $\sim 3 - 5E_k$, where E_k is the breakdown field of air at standard temperature and pressure. To generate significant field enhancement, the density of an initial seed should be comparable to the density inside a streamer channel, which is $10^{12} - 10^{14} \text{ cm}^{-3}$ in atmospheric air. In [53], the possible sources of such strong preionization at 70 km altitude are discussed. It is still an open question where these seeds would come from in atmospheric air, for example to start lightning discharges [51].

Below we first present two examples of seeds that enhance the field sufficiently for positive streamers to form in our particle model. Then we investigate the effect of electron detachment and natural background ionization on the formation process. We again use dry air at 1 bar and 293 Kelvin with a density of 10^4 ions per cm^3 .

4.2. Boundary conditions for the simulations below breakdown

The computational domain that we use for the simulations in background fields below breakdown is shown in Figure 6. Because we want to study the development of a single, isolated streamer discharge, we cannot use periodic boundary conditions as we did in section 3. Instead, an additional grid is introduced, to be able to set boundary conditions for the electric potential farther away. The complete computational domain thus has two parts: an interior grid of $5 \times 5 \times 10 \text{ mm}^3$, in which we use the particle model, and a four times larger grid around it that is used to set the boundary conditions for the electric potential on the interior grid. Dirichlet boundary conditions are imposed on the sides of the larger grid to get a homogeneous background field $E_0 < E_k$ in the vertical direction. Inside the interior grid we use adaptive mesh refinement, so that the strong electric fields around streamer heads can be resolved.

4.3. Streamer inception from conductive seeds

We present results for two initial seeds here, that are both placed at the center of the domain.

4.3.1. First seed The first seed we use is a long, neutral ionized column. The peak ion and electron density is $1.3 \times 10^{13} \text{ cm}^{-3}$. In the two lateral directions, the distribution of electrons and ions is Gaussian, with a width of 0.2 mm. The distribution of plasma in the vertical direction is uniform over a length of 4 mm; at the endpoints there is again a Gaussian distribution. An external electric field of $\sim 0.5E_k$ is applied in the vertical direction. This seed is similar to the initial condition that was used in a 2D fluid model [51], but then scaled to ground pressure.

Figure 7 shows how this seed develops further in the simulations. The ionized column rapidly gets polarized, because the electrons drift against the electric field. A negative and positive charge layer emerge at the top and bottom of the column, respectively. After $\sim 10 \text{ ns}$, a positive streamer forms at the upper end of the column, as shown in the first row of Figure 7. At the lower end, electrons spread out or attach

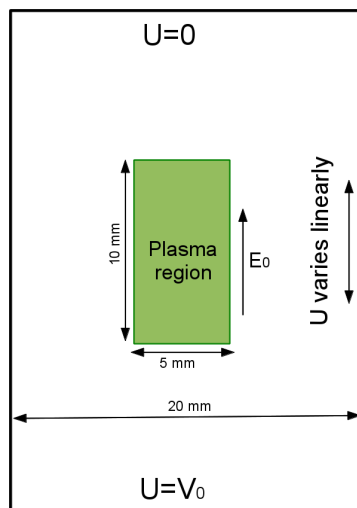


Figure 6. Schematic of the computational domain in the undervolted simulations. The simulated plasma region is embedded in a 4 times larger system. The potential of the large volume is calculated first, then the result is interpolated to get the boundary potential of the small domain. Dirichlet boundary conditions are used at all the boundaries.

to neutral molecules. On the time scales that can be simulated with our particle model, we have not observed negative streamers emerging. An important difference between positive and negative streamers is that positive streamers grow from electrons drifting inwards towards their head, while negative streamers grow from the electrons drifting outwards. Thus, the space charge layer of a positive streamer head is formed by rather immobile ions, while the space charge layer of a negative streamer head is formed by mobile electrons. Negative streamers are therefore typically wider and more diffusive, with less field enhancement, and they do not form as easily [19].

4.3.2. Second seed The second seed has an isotropic Gaussian distribution for electrons and ions in three spatial dimensions. Such seeds have frequently been used to study the formation of positive streamers in point-to-plane gaps [54, 55, 56]. The Gaussian distribution we use here has a peak density of $2.3 \times 10^{13} \text{ cm}^{-3}$ and a width of 0.3 mm. A homogeneous electric field of $\sim 0.7E_k$ is applied in the upward direction. to reduce the simulation time.

Figure 8 shows the evolution of the electron density and the electric field. The development is similar to figure 7: the seed is rapidly polarized and two charge layers form. When the maximum electric field reaches $\sim 3E_k$ at the upper tip, a positive streamer emerges and propagates upward. As before, we do not observe negative streamers on this time scale.

4.3.3. Discussion Both seeds have an electron density comparable to a streamer channel, so it is no surprise that a streamer can develop. The elongated seed causes stronger field enhancement, and therefore positive streamers form more easily than with

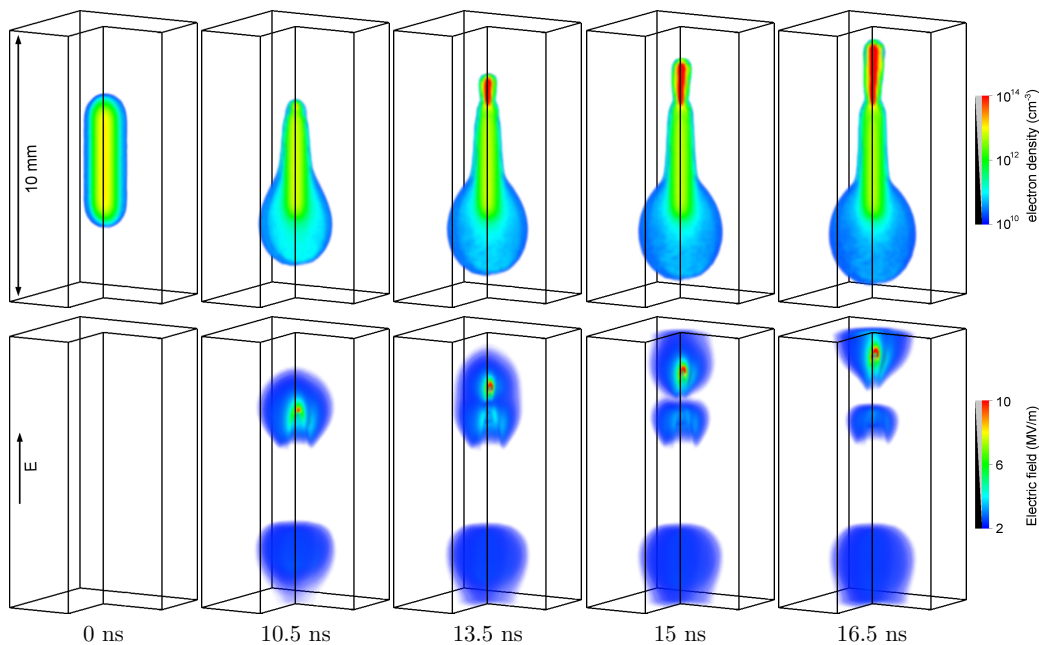


Figure 7. The electron density (top row) and the electric field (bottom row) in a 3D particle simulation with photoionization and natural background ionization (10^4 cm^{-3}). Times are indicated below each column. The simulation starts from an ionized column, with a length of 4 mm, a characteristic width of 0.2 mm and a peak plasma density of $1.3 \times 10^{13} \text{ cm}^{-3}$. The gas and plots were set up in the same way as that for Figure 3, but in an upward homogeneous electric field of 1.7 MV/m (about 0.5 times E_k). The simulation domain has a length of 10 mm in the vertical direction and of 5 mm in the two lateral directions.

the isotropic Gaussian seed. In general, the following can be said about such ionized seeds. First, the seed has to be sufficiently conductive, so that the electric field in its interior gets reduced, and the electric field at its boundary gets enhanced. The required electron density for this is approximately that of a streamer. Second, the longer the seed size is in the direction of the applied electric field, the stronger the field enhancement is at the endpoints. For a conducting sphere, the enhancement factor over the background field is three, but for more elongated shapes it can be much higher. We did not systematically explore which seeds can cause streamer inception under what conditions, because such simulations are very time consuming with our 3D particle model.

4.4. The role of detachment and natural background ionization for streamer inception

Above we have seen that an conductive seed can provide enough field enhancement for positive streamers to start. However, for the start of a discharge not only a high field is required, but also some free electrons. With the ionized seeds presented above, there are many free electrons present in the simulation. But the field enhancement at the

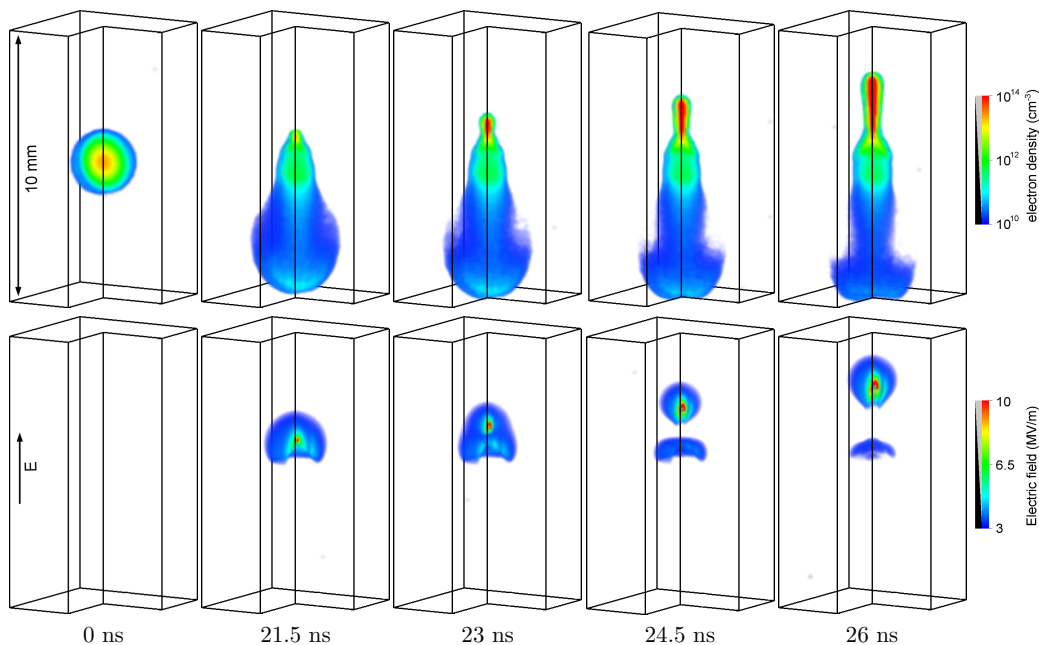


Figure 8. The distributions of electron density (top row) and electric field (bottom row) in a 3D particle model with photoionization and natural background ionization (10^4 cm^{-3}). Times are indicated below each column. The simulation starts from a neutral Gaussian plasma seed, with a characteristic radius of 0.3 mm and a peak plasma density of $2.3 \times 10^{13} \text{ cm}^{-3}$. Gas, simulated domain and plots were set up in the same way as that in Figure 7, but in an upward homogeneous electric field of 2.5 MV/m (about 0.7 times E_k).

positive side of these seeds happens because electrons have moved away from there, so with just the seed it is still hard to start a discharge. Here, we investigate how electron detachment can provide the free electrons to start a discharge. We use the ionized column that was introduced in Section 4.3.1 in a field of $0.5 E_k$. In Figure 9, the position of the streamer head is shown versus time, for three different scenarios:

- (1) Without electron detachment, including only photoionization
- (2) With an initial O_2^- density of 10^4 cm^{-3}
- (3) With an initial O_2^- density of 10^7 cm^{-3}

We observe that positive streamers form a bit earlier if we include the detachment process, but that the density of O_2^- molecules has little influence. The reason is that the initial seed has an electron density orders of magnitude higher than the O_2^- density. Therefore, it is mostly electron attachment at the beginning of the simulation, when the field is still low, that determines the actual O_2^- density. When the field has become large enough for detachment, the discharge can start faster due to the extra detaching electrons.

On the other hand, we observe that electron detachment has no effect on the propagation of the positive streamer. The reason is that photoionization produces most

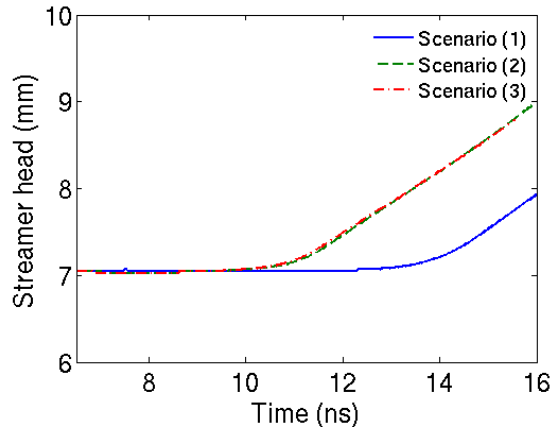


Figure 9. The vertical position of the streamer head as a function of time, see figure 7. We define the position of the head as the location where electric field in vertical direction is maximal. The seed and the background electric field are the same as in Section 4.3.1. Three scenarios are tested: (1) Without electron detachment, so only including photoionization; (2) With an initial O_2^- density of 10^4 cm^{-3} ; (3) With an initial O_2^- density of 10^7 cm^{-3} .

free electrons ahead of the front after the discharge has started [15].

4.5. Comparison with 2D fluid models

In fields above the breakdown threshold, our 3D particle simulations were very different from previous simulations with 2D plasma fluid models. An important factor for this difference was the inclusion of O_2^- ions due to background ionization, from which electrons could detach. On the other hand, in fields below breakdown, our results were in agreement with typical 2D fluid simulations. The reason is that electron impact ionization and electron detachment occur almost only where the field is above breakdown. When the background field is above breakdown, these processes can happen anywhere, and a global discharge forms. But when the background field is below breakdown, these processes happen where the field is locally enhanced: at the streamer head. Around the positive streamer head photoionization will typically be the dominant source of free electrons, so background ionization and electron detachment are not so important.

5. Conclusion

We have studied pulsed discharge formation in electric fields above and below the breakdown threshold with a 3D particle model for air at standard temperature and pressure. Photoionization, a natural level of O_2^- ions due to background ionization and electron detachment were included.

In background electric fields above breakdown, we see discharges distributed over

the whole domain instead of the ‘double-headed’ streamers often appearing in other publications. The major cause for this difference is the inclusion of background ionization and detachment. Free electrons appear at many different places due to detachment from O_2^- ions, and start electron avalanches. These avalanches interact and overlap, and can eventually screen the electric field in the interior of the discharge. This process is analyzed in a separate paper [50].

In background electric fields below the breakdown value, positive streamers can form if the field is locally sufficiently enhanced. We have shown two examples in which an conductive seed of electrons and ions causes sufficient field enhancement for a positive streamer to grow. Negative streamers do not appear in our particle simulations. In fields below breakdown, our 3D particle model gives similar results as the 2D plasma fluid models used by other authors. The reason is that electron detachment and impact ionization only occur around the streamer head, where the field is enhanced. Since photoionization is the dominant source of free electrons around the streamer head, electron attachment and detachment are only important during the inception phase of the discharge.

Acknowledgments

ABS acknowledges the support by an NWO Valorization project at CWI and by STW projects 10118 and 12119. JT was supported by STW project 10755.

References

- [1] Samaranyake W J M, Miyahara Y, Namihira T, Katsuki S, Sakugawa T, Hackam R and Akiyama H 2000 Pulsed streamer discharge characteristics of ozone production in dry air *IEEE Transactions on Dielectrics and Electrical Insulation* **7** 254-60
- [2] Ryo O and Tetsuji O 2007 Ozone production process in pulsed positive dielectric barrier discharge *J. Phys. D: Appl. Phys.* **40** 176
- [3] van Veldhuizen E M 2000 Electrical Discharges for Environmental Purposes: Fundamentals and Applications *New York: Nova Science Publishers*
- [4] van Heesch E J M, Winands G J J and Pemen A J M 2008 Evaluation of pulsed streamer corona experiments to determine the O* radical yield *J. Phys. D: Appl. Phys.* **41** 234015
- [5] Grabowski L, van Veldhuizen E, Pemen A J M and Rutgers W 2006 Corona above water reactor for systematic study of aqueous phenol degradation *Plasma Chem. Plasma Process* **26** 3 - 17
- [6] Winands G J J, Yan K P, Pemen A J M, Nair S A, Liu Z and van Heesch E J M 2006 An industrial streamer corona plasma system for gas cleaning *IEEE Trans. Plasma Sci.* **34** 2426 -33
- [7] Starikovskiy A and Aleksandrov N 2013 Plasma-assisted ignition and combustion *Progress in energy and combustion science* **39** 61-110
- [8] Nijdam S, Van de Wetering F M J H, Blanc R, Van Veldhuizen E M and Ebert U 2010 Probing photo-ionization: Experiments on positive streamers in pure gases and mixtures *J. Phys. D: Appl. Phys.* **43** 145204
- [9] Nijdam S, Wormeester G, Van Veldhuizen E M and Ebert U 2011 Probing background ionization: Positive streamers with a varying pulse repetition rate and with a radioactive admixture *J. Phys. D: Appl. Phys.* **44** 455201
- [10] Van Veldhuizen E M and Rutgers W R 2002 Pulsed positive corona streamer propagation and branching *J. Phys. D: Appl. Phys.* **35** 2169
- [11] Van Veldhuizen E M and Rutgers W R 2003 Inception behavior of pulsed positive corona in several gases *J. Phys. D: Appl. Phys.* **36** 2692-6
- [12] Yi W J and Williams P F 2002 Experimental study of streamers in pure N₂ and N₂/O₂ mixtures and a 13 cm gap *J. Phys. D: Appl. Phys.* **35** 205
- [13] Dubrovin D, Nijdam S, Van Veldhuizen E M, Ebert U, Yair Y and Price C 2010 Sprite discharges on Venus and Jupiter-like planets: A laboratory investigation *J. Geophys. Res.* **115** A00E34
- [14] Hegeler F and Akiyama H 1997 Spatial and temporal distributions of ozone after a wire-to-plate streamer discharge *IEEE Trans. Plasma Sci.* **25** 1158 - 65
- [15] Wormeester G, Pancheshnyi S, Luque A, Nijdam S and Ebert U 2010 Probing photo-ionization: Simulations of positive streamers in varying N₂ : O₂-mixtures *J. Phys. D: Appl. Phys.* **43** 505201
- [16] Celestin S, Bonaventura Z, Zeghondy B, Bourdon A and Segur P 2009 The use of the Ghost Fluid Method for Poissons equation to simulate streamer propagation in point-to-plane and point-to-point geometries *J. Phys. D : Appl. Phys.* **42** 065203
- [17] Tholin F and Bourdon A 2013 Simulation of the stable quasi-periodic glow regime of a nanosecond repetitively pulsed discharge in air at atmospheric pressure *Plasma Sources Sci. Technol.* **22** 045014
- [18] Yair Y, Takahashi Y, Yaniv R, Ebert U and Goto Y 2009 A study on the possibility of sprites in the atmospheres of other planets *J. Geophys. Res.* **114** E09002
- [19] Luque A, Ratushnaya V and Ebert U 2008 Positive and negative streamers in ambient air: modeling evolution and velocities *J. Phys. D: Appl. Phys.* **41** 234005
- [20] Luque A, Ebert U and Hundsdorfer W 2008 Interaction of streamers in air and other oxygen-nitrogen mixtures *Phys. Rev. Lett.* **101** 075005
- [21] Aleksandrov N L and Bazelyan E M 1996 Simulation of long-streamer propagation in air at atmospheric pressure *J. Phys. D: Appl. Phys.* **29** 740-52
- [22] Naidis G V 2012 Simulation of a single streamer traveling along two counterpropagating helium jets in ambient air *IEEE Trans. Plasma Sci.* **40** 2866-9
- [23] Babaeva N Y and Naidis G V 1998 Two-dimensional modeling of positive streamer propagation

- in flue gases in sphere-plane gaps *IEEE Trans. Plasma Sci.* **26** 41-5
- [24] Dhali S K, Williams P F 1985 Numerical simulation of streamer propagation in nitrogen at atmospheric pressure *Phys. Rev. A* **31** 1219-22
- [25] Kossyi I, Kostinsky A Y, Matveyev A A and Silakov V P 1992 Kinetic scheme of the non-equilibrium discharge in nitrogen-oxygen mixtures *Plasma Sources Sci. Technol.* **1** 207-20
- [26] Gordillo-Vazquez, F J 2008 Air plasma kinetics under the influence of sprites *J. Phys. D: Appl. Phys.* **41** 234016
- [27] Luque A and Gordillo-Vazquez F J 2012 Mesospheric electric breakdown and delayed sprite ignition caused by electron detachment *Nature Geoscience* **5** 22-5
- [28] Liu N Y 2012 Mesospheric Multiple ion species fluid modeling of sprite halos and the role of electron detachment of O^- in their dynamics *J. Geophys. Res.* **117** A03308
- [29] Gurevich A V and Karashtin A N 2013 Runaway breakdown and hydrometeors in lightning initiation *Phys. Rev. Lett.* **110** 185005
- [30] Li J B and Cummer S 2012 Relationship between sprite streamer behavior and lightning-driven electric fields *J. Geophys. Res.* **117** A01317
- [31] Sun A B, Teunissen J and Ebert U 2013 Why single streamers do not exist in fields above breakdown in atmospheric air *Geophys. Res. Lett.* **40** 2417-22
- [32] Birdsall C K and Langdon A B 1991 Plasma physics via computer simulation *Bristol: Institute of Physics Publishing*
- [33] Pitchford L C and Boeuf J P 2011 The siglo database <http://www.lxcat.laplace.univ-tlse.fr/database.php>
- [34] Nanbu K 2000 Probability theory of electron-molecule, ion-molecule, molecule-molecule and coulomb collisions for particle modeling of materials processing plasmas and cases *IEEE Trans. Plasma Sci.* **28** 971 - 90
- [35] Teunissen J and Ebert U 2014 Controlling the weights of simulation particles: adaptive particle management using *k-d* trees *J. Comput. Phys.* **259C** 318-30
- [36] Adams J P, Swarztrauber P N, Sweet R 2011 FISHPACK90 <http://www.cisl.ucar.edu/css/software/fishpack90/>
- [37] Montijn C, Ebert U and Hundsdorfer W 2006 An adaptive grid refinement strategy for the simulation of negative streamers *J. Comput. Phys.* **219** 801-35
- [38] Chanrion O and Neubert T 2008 A PIC-MCC code for simulation of streamer propagation in air *J. Comput. Phys.* **227** 7222-45
- [39] Li C, Ebert U and Hundsdorfer W 2011 Simulated avalanche formation around streamers in an overvolted air gap *IEEE Trans. Plasma Sci.* **39** 2256-7
- [40] Zhelezniak M B, Mnatsakanian A K and Sizykh S V 1982 Photo-ionization of nitrogen and oxygen mixtures by radiation from a gas discharge *High Temp.* **20** 357-62
- [41] Luque A and Gordillo-Vazquez F J 2011 Sprite beads originating from inhomogeneities in the mesospheric electron density *Geophys. Res. Lett.* **38** L04808
- [42] Pancheshnyi S 2005 Role of electronegative gas admixtures in streamer start, propagation and branching phenomena *Plasma Sources Sci. Technol.* **14** 645
- [43] Popov N A 2010 Evolution of the negative ion composition in the afterglow of a streamer discharge in air *Plasma Phys. Rep.* **36** 812-8
- [44] Pasko V P, Inan U S and Bell T F 1998 Spatial structure of sprites *Geophys. Res. Lett.* **25** 2123-6
- [45] Liu N Y and Pasko V P 2004 Effects of photoionization on propagation and branching of positive and negative streamers in sprites *J. Geophys. Res.* **109** A04301
- [46] Qin J Q, Celestin S and Pasko V P 2012 Formation of single and double-headed streamers in sprite-halo events *Geophys. Res. Lett.* **39** L05810
- [47] Pasko V P 2007 Red sprite discharges in the atmosphere at high altitude: the molecular physics and the similarity with laboratory discharges *Plasma Sources Sci. Technol.* **16** S13-S29
- [48] Bourdon A, Pasko V P, Liu N Y, Celestin S, Sgur P and Marode E 2007 Efficient models for photoionization produced by non-thermal gas discharges in air based on radiative transfer and the

- Helmholtz equations *Plasma Sources Sci. Technol.* **16** 656-78
- [49] Bessires D, Paillol J, Bourdon A, Sgur P and Marode E 2007 A new one dimensional moving mesh method applied to the simulation of streamer discharges *J. Phys. D : Appl. Phys.* **40** 6559-70
- [50] Teunissen J, Sun A B, Ebert U, A time scale for electrical screening in pulsed gas discharges, submitted to *J. Phys. D : Appl. Phys.*
- [51] Liu N Y, Kosar B, Sadighi S, Dwyer J R and Rassoul H K 2012 Formation of streamer discharges from an isolated ionization column at sub-breakdown conditions *Phys. Rev. Lett.* **109** 025002
- [52] Bazelyan E M and Raizer Y P 1998 *Spark discharge* (New York: Chemical Rubber Company Press)
- [53] Kosar B C, Liu N Y and Rassoul H K 2012 Luminosity and propagation characteristics of sprite streamers initiated from small ionospheric disturbances at subbreakdown conditions *J. Geophys. Res.* **117** A08328
- [54] Kulikovskiy A A 1998 Positive streamer in a weak field in air: A moving avalanche-to-streamer transition *Phys. Rev. E* **57** 7066-74
- [55] Serdyuk Y V, Larsson A, Gubanski S M and Akyuz M 2001 The propagation of positive streamers in a weak and uniform background electric field *J. Phys. D: Appl. Phys.* **34** 614-23
- [56] Bonaventura Z, Bourdon A, Celestin S and Pasko V P 2011 Electric field determination in streamer discharges in air at atmospheric pressure *Plasma Sources Sci. Technol.* **20** 035012